

RETHINKING HUMAN-OBJECT INTERACTION EVALUATION FOR BOTH VISION–LANGUAGE MODELS AND HOI-SPECIFIC METHODS

Qinqian Lei¹ Bo Wang² Robby T. Tan^{1,3}

¹National University of Singapore ²University of Mississippi

³ASUS Intelligent Cloud Services (AICS)

qinqian.lei@u.nus.edu, hawk.rsrch@gmail.com, roddy_tan@asus.com

ABSTRACT

Prior human-object interaction (HOI) detection methods have integrated early vision–language models (VLMs) such as CLIP, but only as supporting components within their frameworks. In contrast, recent advances in large, generative VLMs suggest that these models may already possess strong ability to understand images involving HOI. This naturally raises an important question: can general-purpose standalone VLMs effectively solve HOI detection, and how do they compare with specialized HOI methods? Answering this requires a benchmark that can accommodate both paradigms. However, existing HOI benchmarks such as HICO-DET were developed before the emergence of modern VLMs, and their evaluation protocols require exact matches to annotated HOI classes. This is poorly aligned with the generative nature of VLMs, which often yield multiple valid interpretations in ambiguous cases. For example, a static image may capture a person mid-motion with a frisbee, which can plausibly be interpreted as either “throwing” or “catching”. When only “catching” is annotated, the other, though equally plausible for the image, is marked incorrect when exact matching is used. As a result, correct predictions might be penalized, affecting both VLMs and HOI-specific methods. To avoid penalizing valid predictions, we introduce a new benchmark that reformulates HOI detection as a multiple-answer multiple-choice task, where each question includes only ground-truth positive options and a curated set of negatives that are constructed to reduce ambiguity (e.g., when “catching” is annotated, “throwing” is not selected as a negative to avoid penalizing valid predictions.) The proposed evaluation protocol is the first of its kind for both VLMs and HOI methods, enabling direct comparison and offering new insight into the current state of progress in HOI understanding.

1 INTRODUCTION

Existing human–object interaction (HOI) detection methods utilize vision–language models (VLMs), such as CLIP Radford et al. (2021) and BLIP Li et al. (2022), as feature encoders to supply aligned image–text representations in their frameworks Liao et al. (2022); Ning et al. (2023); Mao et al. (2024); Cao et al. (2024); Yuan et al. (2023). More recently, standalone large generative VLMs (e.g., Qwen2.5-VL Bai et al. (2025), InternVL3 Zhu et al. (2025)) demonstrate promising ability to interpret complex visual scenes, including aspects of HOI Bai et al. (2025); Shahriar et al. (2024); Chen et al. (2024); Yang et al. (2023). In practice, modern VLMs often produce plausible descriptions for HOI even in complex scenes.

Different from the early VLM encoders used within HOI-specific methods, throughout this paper, VLMs refer to being used as standalone models (unless we state it otherwise). This distinction motivates an important question: can general-purpose standalone VLMs, used directly as end-to-end models, perform HOI detection compared to specialized HOI methods Lei et al. (2025); Li et al. (2024a); Kim et al. (2025)? Building on our prior work in HOI detection (e.g., EZ-HOI and HOLa) Lei et al. (2024b;a; 2025), we aim to answer this question, which is important for understanding the true state of progress in HOI detection and for guiding whether future research should

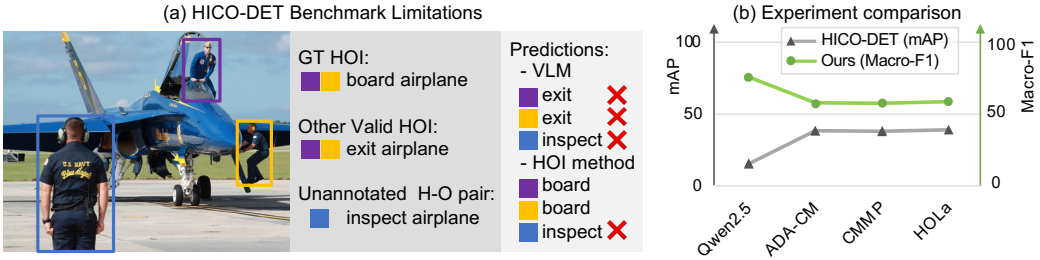


Figure 1: (a) Existing evaluation requires exact match with ground-truth annotations (“board airplane”), but those annotations suffer from incomplete annotations, such as missing interaction label “exit airplane” and the unannotated human-object pairs (the blue-box person and the airplane). (b) Experiment comparison, including Qwen2.5-VL-32B Bai et al. (2025), ADA-CM Lei et al. (2023), CMMMP Lei et al. (2024d), and HOLa Lei et al. (2025), where Qwen2.5-VL-32B is VLM and ADA-CM, CMMMP and HOLa are HOI-specific methods. We compare Macro-F1 metric in our benchmark under *Setting 3* with the Mean Average Precision (mAP) metric in HICO-DET benchmark.

focus on HOI-specific methods or leverage VLMs. Addressing it requires a benchmark that can accommodate both paradigms: general-purpose VLMs and HOI-specific methods.

At first glance, it might seem that existing HOI benchmarks such as HICO-DET Chao et al. (2018) could already serve to compare VLMs and HOI-specific methods, because both VLMs and HOI-specific methods ultimately can output detected boxes and HOI classes. However, these benchmarks were created before the emergence of modern VLMs and rely on evaluation protocols that require exact matches to the annotated HOI classes, rejecting all other possibilities. This is not suitable for VLMs: unlike HOI-specific models that are optimized for a fixed label space, VLMs are generative and can produce multiple valid interpretations in ambiguous scenarios. For example, as shown in Fig. 1(a), the image shows a person about to step into an airplane (purple box) or another climbing the boarding ladder (yellow box). Both can reasonably be interpreted as “boarding” or “exiting,” due to temporal ambiguity. In these cases, the ground-truth annotations are often incomplete, with other plausible interpretations left unannotated. As a result, when only one interpretation is annotated, other equally valid predictions are penalized as errors, leading to an underestimation of model capability, especially for VLMs.

Beyond this, another limitation comes from the sparsity of HOI annotations, especially in multi-person multi-object scenarios. Since HOI tasks involve combinations of actions and objects, the annotation space grows exponentially, making comprehensive labeling particularly difficult in multi-person and multi-object scenes Hou et al. (2020; 2021); Lei et al. (2024b;d). For example, as shown in Fig. 1(a) (the person in the blue box is not annotated in the ground truth), valid interactions for unannotated human-object pairs are inevitably penalized as errors. This issue affects not only VLMs but also HOI-specific methods, since both are evaluated against incomplete ground truths, leading to underestimated performance. Fig. 1(b) further illustrates the overall impact of these limitations. While HOI-specific methods remain below 50% mAP, general-purpose VLMs drop even further to around 16%, underscoring the severity of the open problems in the existing HOI benchmarks.

To address these open problems, we introduce a new benchmark that reformulates HOI detection as a multiple-answer, multiple-choice task. Each question consists of the annotated ground-truth interactions as positive choices and a curated set of negatives. To carefully select these negatives, we apply a multi-stage filtering process with several state-of-the-art VLMs to remove any plausible false negatives. We then retain only those that are inconsistent with the HOIs in the given image, mitigating the risk of including valid but unlabeled interactions, which could otherwise wrongly penalize a model’s performance.

While the multiple-choice reformulation with negative selection alleviates the issue of missing interaction labels, another limitation lies in the sparsity of HOI annotations. Since it is expensive and laborious to exhaustively annotate all human-object pairs, especially in multi-person scenarios, unannotated pairs are present in existing benchmarks. To avoid penalizing predictions on unannotated human-object pairs, we introduce a setting in our benchmark (i.e., *Setting 2*) where the person of interest is specified, allowing the model to focus on individual HOI recognition. At the same

time, it is important to evaluate a model’s detection ability, as well as its capacity to understand various interactions in multi-person scenes. For the above reasons, we propose three complementary evaluation settings in total: *Setting 1* full-scene HOI recognition, which tests whether a model can understand all interactions in an image, with curated negatives designed to mitigate the penalization of unannotated human-object pairs; *Setting 2* per-person HOI recognition with the bounding box provided, which assesses localized understanding while avoiding detection errors; and *Setting 3* joint detection and recognition ability evaluation.

In summary, our work makes the following contributions:

- We introduce the first evaluation benchmark suitable for both standalone general-purpose VLMs and HOI-specific methods, reformulating HOI detection as a multiple-answer, multiple-choice task. This unified approach resolves limitations of existing benchmarks, such as missing annotations and ambiguity.
- Our benchmark evaluates multiple state-of-the-art VLMs and HOI detection methods, providing a more accurate view of current performance and overcoming the unreliable evaluation protocols of existing benchmarks.

2 NEW BENCHMARK

2.1 PRELIMINARY

Base Dataset We build our benchmark based on HICO-DET Chao et al. (2018), the widely used dataset for HOI detection Tamura et al. (2021); Wu et al. (2023); Hou et al. (2020); Yuan et al. (2022); Tu et al. (2023). HICO-DET provides 9,658 test images covering 600 HOI classes. Each annotation specifies a human bounding box, an object bounding box, and their associated interaction label, e.g., ⟨person, ride, bicycle⟩. HOI-specific methods are thus required to output a set of such triplets, consisting of detected bounding boxes of human–object pairs and predicted HOI classes.

Among the 600 HOI classes, we identified 68 classes that are closely related to temporal ambiguity, where static images can be inherently ambiguous as it may not fully capture the temporal dynamics of the interaction (e.g., “boarding” vs. “exiting”), and thus pose challenges for existing HOI evaluation. Detailed list of HOI classes and its discussion are provided in Appendix A. In addition, out of the 9,658 test images in HICO-DET, around 5,040 images were identified as containing multiple people by Qwen2.5-VL-32B Bai et al. (2025). As prior work has shown Gupta et al. (2019); Niitani et al. (2019); Zhang et al. (2019); Suri et al. (2023), exhaustive annotation in multi-person scenes is already challenging for vision tasks such as pose estimation and detection. This challenge becomes even more severe in HOI detection, where annotations involve combinations of humans and objects, and the number of possible pairs grows quadratically Hou et al. (2020); Lei et al. (2024d), making comprehensive labeling particularly difficult and further amplifying the limitations of the existing benchmark. In our benchmark, we reuse these annotations to construct evaluation questions. However, unlike the original evaluation protocol, our benchmark can avoid being negatively influenced by incomplete annotation issues by our negative choice construction to select reliable negative set, ensuring that missing valid labels do not lead to unfair penalties.

Traditional Evaluation Metric The standard evaluation protocol for HOI detection is based on average precision (AP). A prediction is considered correct if the detected human and object boxes match the ground-truth boxes with Intersection over Union (IoU) greater than 0.5, and the predicted HOI classes exactly match the ground truths. For HICO-DET Chao et al. (2018), results are reported as mean AP (mAP) over 600 HOI classes. V-COCO Lin et al. (2014) adopts the same evaluation criterion on 29 HOI classes. The recent SWiG-HOI Wang et al. (2022) also follows this principle and reports mAP across its defined 5,500 HOI classes. Despite differences in label space, all existing benchmarks rely on exact-match evaluation, which becomes problematic under incomplete and ambiguous annotations.

2.2 BENCHMARK CONSTRUCTION

Task Reformulation To overcome the limitations of exact-match evaluation, we reformulate HOI detection as a multiple-answer, multiple-choice task. For one human–object pair in an image, we

construct a question with four choices, and the model must select all correct ones. Since a single person may be involved in multiple valid interactions (e.g., hold knife and cut with knife), a question may contain more than one positive answer. Ground-truth annotations provide the positive choices, while the negative choices are curated to be semantically distinct from the interactions in the image. Our approach avoids penalizing valid but unlabeled interactions and ensures a more reliable evaluation of HOI performances.

Negative Choice Construction The central challenge lies in constructing reliable negative choices. We first build a candidate pool by collecting all actions associated with the objects that a person interacts with (e.g., for bicycle, possible actions include ride, hold, carry, etc.). Ground-truth labels for the given person–object pair are removed from this pool, leaving only potential negatives. To eliminate potential false negatives, we employ a two-stage filtering process with state-of-the-art VLMs. In the first stage, GPT-4.1 OpenAI (2023) groups all candidates into two sets: one semantically consistent with the image and one inconsistent. We retain only the inconsistent group as candidates. In the second stage, we further refine the retained negatives using another VLM, Qwen2.5-VL-32B Bai et al. (2025). A potential concern is that Qwen2.5-VL is also one of the models evaluated, which might raise the possibility of bias if its judgments shaped the benchmark. We address this explicitly: If the VLM judges a candidate as negative, we directly accept it, since our quality check (i.e., based on 200 sampled cases) confirmed that its negative judgments are reliable. However, when the VLM labels a candidate as positive, this does not necessarily mean it is true, as it may reflect that the model finds the case difficult and misclassifies a negative as positive. If such cases were removed, the benchmark would unintentionally discard the “hard negatives” for the second VLM (Qwen2.5-VL), introducing bias and making the evaluation unfairly favorable to it. To avoid this, we pass all candidates that Qwen2.5-VL marks as positive to a third VLM, GPT-4o Hurst et al. (2024), an independent model family, for final checking. This ensures that the generated negative choices are not biased toward a particular VLM and suitable for evaluating the HOI performance of various VLMs. In addition, we conduct a quality check by randomly sampling 200 images, verifying that all of them contain valid negative choices.

Each question uses a fixed four-choice format for consistent comparability across models, allows multiple correct answers, and randomizes the option order at evaluation time. Randomization is necessary to avoid positional bias, since prior work Pezeshkpour & Hruschka (2024); Zheng et al. (2024) shows that large language models (LLMs) are sensitive to the order of options in multiple-choice questions and often exhibit systematic biases (e.g., a tendency to over-select option A).

2.3 BENCHMARK EVALUATION

Evaluation Settings Existing benchmarks suffer from two key issues: missing interaction labels, especially caused by temporal ambiguity, and unannotated human-object pairs, especially in multi-person scenarios where exhaustive labeling of all human–object pairs is laborious. While the multiple-choice reformulation with curated negatives addresses the first issue, the second requires carefully designed evaluation settings to avoid unfairly penalizing unannotated pairs while still assessing different aspects of a model’s capability, such as HOI recognition with and without joint detection. To this end, our benchmark introduces three settings under the same multiple-choice formulation. Each corresponds to a variant of the same image-based question but differs in whether multiple people are considered and whether detection is required. Specifically, we only consider human detection, rather than both human and object, so the model must not only classify the interaction after detection but also identify the corresponding interacted object.

In *Setting 1*, a model predicts interactions for all persons in the image, directly evaluating HOI recognition ability at the full-scene level without scoring detection. For example, in Fig. 2(a), the positive choices include A, B, C, D since one person is carrying a bike and another is riding a bike. Curated negatives are constructed to be inconsistent with HOIs in the image, aiming to mitigate the penalization of predictions for the unannotated individuals. For example, in Fig. 2(c), ground-truth annotation only includes the person in red box, while the other snowboarders in the scene are unannotated. In this case, since negative choices are drawn to be semantically distinct from the HOIs visible in the image, we exclude options such as wearing or holding a snowboard, ensuring that predictions on unannotated individuals are not penalized. In *Setting 2*, the bounding box of a specified person is provided, so unannotated individuals are not considered. This setting evaluates a model’s HOI understanding capability without being affected by human detection errors. In Fig. 2(a), the



Figure 2: Example questions in our new HOI benchmark, illustrated under three evaluation settings. The red boxes are provided for visualization purpose only in *Setting 2* and *3*. In our actual benchmark, questions do not include red boxes in the image but instead specify the person by bounding-box coordinates. *Setting 1*: The model selects interactions for all persons in the image. There are 2 persons in the example. *Setting 2*: The target person’s bounding box is provided, and the model predicts that individual’s interactions. *Setting 3*: The model must first detect the target person; if the detected box overlaps the ground truth ($\text{IoU} \geq 0.5$), it proceeds to predict that person’s interactions.

target is the person carrying a bike, so the positive choices are A, B, C. In *Setting 3*, a model must first detect persons in the image. If a detected box overlaps with the ground-truth box of the target person (i.e., $\text{IoU} \geq 0.5$), the model proceeds to predict that person’s interactions. This setting jointly evaluates both detection and interaction recognition.

Single- and Multi-person Scenarios. To enable finer-grained analysis, we further separate each evaluation setting into single-person and multi-person cases. Single-person cases contain images with only one person, while multi-person cases involve multiple individuals, requiring the model to distinguish different persons’ interactions. Since HOI annotations are often sparse (i.e., not every person in an image is annotated), we adopt a hybrid strategy to split the two cases. Images with multiple annotated persons are directly categorized as multi-person, while images with only a single annotated person are further verified using Qwen2.5-VL-32B Bai et al. (2025) to check whether additional persons are present. This ensures a more reliable split for single- and multi-person scenarios. We also report results under the overall scenario, which aggregates both single- and multi-person cases.

In total, our benchmark contains 9,338 questions, each derived from an annotated image from HICO-DET test set. All three evaluation settings (*Setting 1–3*) are constructed on the same set of 9,338 questions to ensure comparability across settings. For finer-grained analysis, among all questions, 4,538 correspond to images with a single person (single-person scenario), while 4,800 come from images with multiple persons (multi-person scenario).

Evaluation Metrics To evaluate multiple-answer multiple-choice questions, we adopt set-based metrics that compare the predicted and ground-truth label sets directly. These metrics are used in multi-label and question-answering evaluation Rajpurkar et al. (2016); Wu & Zhou (2017). We utilize four complementary measures: Instance-F1, Macro-F1, Micro-F1 and Exact Match Accuracy (EM).

Let Q be the set of all evaluation questions. For each question $q \in Q$, let P_q be the set of predicted interaction labels and G_q be the ground-truth set (i.e., positive choices).

Instance-F1 evaluates performance at the question level. For each question, we compute the F1-score between the predicted and ground-truth label sets, and then average over all questions to measure how well the model performs on an average instance.

$$\text{Instance-F1} = \frac{1}{|Q|} \sum_{q \in Q} \text{F1}(q) = \frac{1}{|Q|} \sum_{q \in Q} \frac{2|P_q \cap G_q|}{|P_q| + |G_q|}. \quad (1)$$

where $|\cdot|$ denotes the number of elements in a set and $P_q \cap G_q$ denotes the overlap between P_q and G_q , the set of correctly predicted labels for question q .

Macro-F1 evaluates the performance in a class-balanced way. Let \mathcal{C} denote the set of HOI classes. For each class $c \in \mathcal{C}$, we compute the F1-score over the questions involving that class, denoted as F1_c . Macro-F1 is then obtained by averaging F1_c across all classes, so that rare and common HOI classes contribute equally.

$$\text{Macro-F1} = \frac{1}{|\mathcal{C}|} \sum_{c \in \mathcal{C}} \text{F1}_c = \frac{1}{|\mathcal{C}|} \sum_{c \in \mathcal{C}} \frac{2 \sum_q \mathbf{1}[c \in P_q \cap G_q]}{\sum_q \mathbf{1}[c \in P_q] + \sum_q \mathbf{1}[c \in G_q]}, \quad (2)$$

where $\mathbf{1}[\cdot]$ denotes the indicator function, which equals 1 if the condition inside holds and 0 otherwise.

Micro-F1 metric aggregates predictions across all questions into a single set, and computes precision and recall globally before deriving the F1-score.

$$\text{Micro-F1} = \frac{2 \sum_q |P_q \cap G_q|}{\sum_q |P_q| + \sum_q |G_q|} \quad (3)$$

Finally, we adopt Exact Match Accuracy (EM), which measures whether the predicted set of interactions for a question exactly matches the ground-truth set. Unlike the exact-match mAP metric in traditional HOI benchmarks, which is negatively affected by incomplete annotations and penalizes unlabeled interactions, our multiple-choice formulation avoids this issue through curated negatives. Thus, EM serves as a complementary metric that strictly measures how often predictions are exactly correct.

$$\text{EM} = \frac{1}{|Q|} \sum_{q \in Q} \mathbf{1}[P_q = G_q]. \quad (4)$$

Together, these four metrics provide a well-rounded evaluation. Instance-F1 captures per-question performance; Macro-F1 balances across classes; Micro-F1 measures overall aggregate performance; and EM reports the proportion of cases where predictions are exactly correct.

3 EXPERIMENTS

3.1 EXPERIMENT SETUP

Baselines We compare our benchmark against two groups of baselines: general-purpose VLMs and HOI-specific methods. Recent large VLMs represent the frontier of general-purpose image understanding. Although not explicitly trained for HOI detection, these models demonstrate strong open-vocabulary grounding, visual and spatial reasoning abilities, which makes them natural candidates

Method	Instance-F1 (%)			Macro-F1 (%)			Micro-F1 (%)			EM (%)		
	Single	Multi	Overall	Single	Multi	Overall	Single	Multi	Overall	Single	Multi	Overall
<i>VLM (small models: 7B / 8B)</i>												
LLaVA-OV-7B	43.47	44.17	43.83	26.11	28.30	28.02	43.77	44.36	44.07	18.36	20.33	19.37
InternVL2.5-8B	42.49	39.18	40.79	50.58	45.55	48.85	54.11	51.90	53.00	23.36	21.58	22.45
InternVL3-8B	80.00	79.79	79.89	72.94	69.49	73.58	78.43	78.32	78.38	51.15	52.90	52.05
Qwen2-VL 7B	25.74	42.35	34.28	32.90	42.24	37.11	34.04	49.06	41.98	10.14	23.13	16.81
Qwen2.5-VL 7B	79.65	79.63	79.64	71.71	69.21	73.33	76.99	77.52	77.26	47.58	48.13	47.86
<i>VLM (large models: 32B / 38B)</i>												
InternVL3-38B	83.19	82.27	82.72	75.89	73.21	77.01	81.25	80.79	81.02	56.52	56.83	56.68
Qwen2.5-VL 32B	85.85	83.37	84.57	76.36	71.18	76.21	84.78	82.57	83.65	57.10	52.50	54.73
<i>HOI-specific methods</i>												
ADACM	73.40	65.67	69.42	60.61	56.96	60.27	83.95	78.19	81.18	39.55	16.08	27.49
CMMMP	72.67	65.34	68.90	60.60	56.85	60.21	83.16	78.05	80.72	39.29	16.23	27.44
LAIN	70.80	63.96	67.28	57.69	54.45	57.44	81.44	76.50	79.09	38.08	17.44	27.47
HOLA	73.08	65.99	69.44	62.03	57.15	60.84	83.31	78.12	80.83	39.82	16.94	28.06
CMDSE	76.02	65.21	70.46	57.69	49.44	55.02	84.88	76.57	80.88	50.26	19.73	34.57

Table 1: *Setting 1* experiment results comparison. Results are reported for VLMs (small vs. large) and HOI-specific methods. Best performance within each group is highlighted in **bold**. “Single” denotes single-person scenarios, “Multi” denotes multi-person scenarios, and “Overall” denotes the aggregate of both.

for HOI evaluation. Qwen2-VL and Qwen2.5-VL (7B / 32B) Bai et al. (2025) are selected as they excel in fine-grained spatial localization and visual reasoning, making them suitable for HOI tasks. InternVL2.5 and InternVL3 (8B / 38B) Chen et al. (2024); Wang et al. (2024b); Zhu et al. (2025) are included because they achieve leading performance across diverse multimodal benchmarks and emphasize high-resolution perception, which is relevant for recognizing human–object interactions. LLaVA-OV-7B Li et al. (2025) is an instruction-tuned VLM designed for open-vocabulary understanding.

We further compare with recent HOI detection methods. ADA-CM Lei et al. (2023), CMMMP Lei et al. (2024d), LAIN Kim et al. (2025) and HOLA Lei et al. (2025) demonstrate competitive performance on the existing HICO-DET benchmark Chao et al. (2018). In addition, CMD-SE Lei et al. (2024c) is a recent open-vocabulary HOI detection method emphasizing generalization ability, achieving competitive performance on SWiG-HOI Wang et al. (2022) and HICO-DET benchmarks. We use best-performing pre-trained checkpoints when available, and otherwise reproduce results with the authors’ code under the closest available configurations. Specifically, ADA-CM, CMMMP, and HOLA are evaluated with the ViT-L vision backbone, while CMD-SE and LAIN are based on ViT-B.

Implementation Details For general-purpose VLMs, we provide the question prompt along with an explicit answer-format instruction: “IMPORTANT: Reply with the letter(s) ONLY, separated by commas if multiple. For example, if the correct answers are (A) and (B), your output must be: A,B. Do NOT include any brackets or other symbols.” We then parse the model outputs accordingly and evaluate each prediction. For HOI-specific methods, we take their top-5 predictions for each question and check whether these match any of the provided choices, following the standard top-5 evaluation used in ImageNet Deng et al. (2009). We adopt top-5 rather than top-1, since each of our questions may contain multiple correct answers, while top-10 would be unnecessarily loose.

3.2 QUANTITATIVE RESULTS

Table 1 shows that in *Setting 1*, InternVL3-8B is the best-performing small-size VLM (7B/8B), outperforming the SOTA HOI-specific method on all reported metrics, consistently across single-person, multi-person, and overall scenarios. This demonstrates that even small-size VLMs provide stronger holistic HOI understanding than specialized HOI detection methods under HOI recognition-only evaluation. Scaling VLMs further to 32B/38B yields additional performance gains, confirming

Method	Instance-F1 (%)			Macro-F1 (%)			Micro-F1 (%)			EM (%)		
	Single	Multi	Overall	Single	Multi	Overall	Single	Multi	Overall	Single	Multi	Overall
<i>VLM (small models: 7B / 8B)</i>												
LLaVA-OV-7B	32.76	35.04	33.93	20.96	22.72	21.91	32.79	34.85	33.83	15.93	18.73	17.37
InternVL2.5-8B	45.15	42.08	43.57	50.56	47.99	51.03	59.16	55.58	57.39	23.58	22.63	23.09
InternVL3-8B	81.35	77.83	79.54	72.80	67.49	72.87	80.48	77.42	78.94	48.88	46.63	47.72
Qwen2-VL 7B	65.28	63.77	64.51	60.29	56.42	60.66	63.07	62.14	62.60	35.79	37.17	36.50
Qwen2.5-VL 7B	83.15	81.29	82.19	73.79	69.49	74.04	81.58	79.88	80.73	51.52	50.23	50.86
<i>VLM (large models: 32B / 38B)</i>												
InternVL3-38B	84.09	82.43	83.24	74.37	72.22	75.81	83.14	81.64	82.39	57.60	57.90	57.75
Qwen2.5-VL 32B	88.28	87.37	87.81	79.49	75.51	79.46	87.29	86.34	83.98	63.05	63.10	63.07

Table 2: *Setting 2* experiment results comparison. Results are grouped by VLM size (small vs. large). Best performance within each group is highlighted in **bold**. “Single” denotes single-person scenarios, “Multi” denotes multi-person scenarios, and “Overall” denotes the aggregate of both.

Method	Instance-F1 (%)			Macro-F1 (%)			Micro-F1 (%)			EM (%)		
	Single	Multi	Overall	Single	Multi	Overall	Single	Multi	Overall	Single	Multi	Overall
<i>VLM (small models: 7B / 8B)</i>												
LLaVA-OV-7B	-	-	-	-	-	-	-	-	-	-	-	-
InternVL2.5-8B	22.11	16.47	19.32	31.82	27.19	28.44	34.63	27.76	31.41	7.36	4.88	6.08
InternVL3-8B	29.93	22.13	26.46	40.36	34.56	37.52	41.23	31.92	37.40	6.70	3.79	5.20
Qwen2-VL 7B	-	-	-	-	-	-	-	-	-	-	-	-
Qwen2.5-VL 7B	43.86	59.44	51.22	49.52	63.33	57.39	55.09	68.45	61.60	25.41	29.04	27.28
<i>VLM (large models: 32B / 38B)</i>												
InternVL3-38B	63.50	59.90	61.68	65.92	61.99	65.03	71.47	68.34	69.94	33.43	31.38	32.37
Qwen2.5-VL 32B	83.02	75.16	79.06	76.90	71.86	75.79	85.27	80.46	82.95	52.53	46.04	49.20
<i>HOI-specific methods</i>												
ADACM	70.18	57.18	63.49	58.91	53.27	57.66	82.55	72.70	77.95	44.34	36.69	40.40
CMMP	69.42	56.43	62.74	58.89	53.22	57.52	81.76	72.28	77.36	43.81	36.79	40.20
LAIN	67.66	55.99	61.66	55.95	51.09	54.99	80.14	71.73	76.24	41.49	37.65	39.52
HOLa	69.96	57.81	63.71	60.54	53.91	58.59	81.97	73.15	77.86	44.42	38.67	41.46
CMDSE	69.91	49.96	59.66	54.77	43.40	50.12	81.74	66.18	74.58	49.18	31.21	39.94

Table 3: *Setting 3* experiment results comparison. Results are grouped by VLM size (small vs. large) and HOI-specific methods. Best performance within each group is highlighted in **bold**. “Single” denotes single-person scenarios, “Multi” denotes multi-person scenarios, and “Overall” denotes the aggregate of both.

that VLMs surpass HOI-specific methods in *Setting 1*. Table 1 highlights that VLMs can reliably recognize HOIs when detection error is not considered, particularly on Macro-F1 and Exact-Match Accuracy (EM).

Table 2 reports only VLM results, since HOI-specific methods inherently detect human–object pairs and therefore cannot take advantage of the provided ground-truth bounding boxes. The results show that when the target person is provided, Qwen2.5-VL-7B achieve consistently stronger performance compared to *Setting 1*, showing that comprehensive HOI understanding across the full scene remains challenging. Scaling up further improves performance, with Qwen2.5-VL-32B delivering the best overall performance and surpassing InternVL3-38B by a clear margin. Comparing Table 1 and Table 2, we observe that InternVL3 performs better in *Setting 1*, indicating better capability in overall HOI understanding, whereas Qwen2.5-VL achieves higher scores in *Setting 2*, reflecting more accurate recognition of individual HOIs when the person of interest is specified.

Table 3 evaluates the whole HOI detection process, where models must both localize persons and recognize interactions. Among small VLMs, Qwen2.5-VL-7B achieves the highest performance, while scaling up to 32B further improves results, with Qwen2.5-VL-32B outperforming InternVL3-

Method	Instance-F1			Macro-F1			Micro-F1			EM Acc.		
	Single	Multi	Overall									
<i>VLM (small models: 7B / 8B)</i>												
LLaVA-OV-7B	33.02	34.76	33.91	21.02	22.78	21.89	32.98	34.63	33.81	15.76	17.40	16.60
InternVL2.5-8B	44.66	41.64	43.11	51.39	45.40	50.05	58.78	55.82	57.31	23.56	22.23	22.87
InternVL3-8B	80.62	76.14	78.31	73.97	67.92	73.30	80.38	77.11	78.74	48.19	45.48	46.80
Qwen2-VL 7B	64.33	61.53	62.89	59.17	57.33	60.54	62.63	61.07	61.85	34.95	35.17	35.06
Qwen2.5-VL 7B	81.52	78.08	79.75	73.22	70.31	73.87	81.16	78.92	80.04	49.91	49.27	49.58
<i>VLM (large models: 32B / 38B)</i>												
InternVL3-38B	83.11	79.23	81.12	75.14	70.31	75.81	82.97	80.37	81.67	57.78	55.60	56.67
Qwen2.5-VL 32B	87.08	83.79	85.39	79.73	73.80	78.81	86.92	84.83	85.87	63.11	59.52	61.27

Table 4: *Setting 3* experiment results comparison with off-the-shelf detector (DETR) Carion et al. (2020). Results are grouped by VLM size (small vs. large). Best performance within each group is highlighted in **bold**. “Single” denotes single-person scenarios, “Multi” denotes multi-person scenarios, and “Overall” denotes the aggregate of both.

38B across all metrics. Overall, VLM results are lower than in *Setting 2*, highlighting the additional difficulty introduced by the detection step. HOI-specific methods remain competitive with small-size VLMs, often surpassing them by large margins. They also achieve comparable results to large-size VLMs in Micro-F1 and EM accuracy, but generally fall behind in Macro-F1 and Instance-F1. This suggests that HOI-specific methods perform well on many test cases but struggle to maintain balanced performance across all HOI classes, whereas large VLMs exhibit more consistent recognition across categories. One possible explanation is that HOI-specific methods are trained on relatively small and imbalanced HOI datasets, which may bias toward certain classes, however, VLMs benefit from large-scale pretraining on diverse vision–language data and may therefore suffer less from such imbalance.

Since VLMs often struggle with reliable person detection, we follow the two-stage HOI detection paradigm Lei et al. (2023); Wang et al. (2024a); Zhang et al. (2022) and leverage a widely used off-the-shelf object detector, a DETR model Carion et al. (2020) pre-trained on HICO-DET. Table 4 shows that incorporating DETR helps improve performance in the *Setting 3* evaluation, though remains lower than in *Setting 2* due to detection errors. Among small models, Qwen2.5-VL-7B achieves the best overall performance across all metrics. For large models, Qwen2.5-VL-32B consistently outperforms InternVL3-38B. These results confirm that the detection ability of recent VLMs remains inferior to that of specialized off-the-shelf object detectors.

Note that the overall scenario (i.e., combining Single- and Multi-person scenarios) may occasionally yield higher Macro-F1 than its subsets, as explained in detail in Appendix B.

4 RELATED WORK

HOI detection methods. HOI detection methods can be categorized into two-stage and one-stage approaches. Two-stage methods first detect humans and objects, then classify interactions for paired boxes Zhang et al. (2021; 2022); Park et al. (2023); Hou et al. (2022). In contrast, one-stage methods directly predict \langle human, object, verb \rangle triplets in an end-to-end manner Zou et al. (2021); Tamura et al. (2021); Qu et al. (2022); Tu et al. (2023); Li et al. (2024b). Despite the progress, current evaluation benchmarks rely on exact matches to annotated HOIs, which requires the availability of exhaustive labeling of all human–object pairs in given images. However, annotations in existing benchmarks are sparse, especially in multi-person scenes, so plausible but unlabeled interactions are penalized, leading to underestimated performance (e.g., below 50% mAP on HICO-DET for SOTA HOI methods). Our benchmark mitigates this by reformulating evaluation as multiple-choice question with curated negatives, avoiding penalizing a model’s plausible predictions that are not annotated in ground truths.

Existing HOI benchmarks. HICO-DET provides HOI annotations across 600 classes (117 verbs and 80 objects) Chao et al. (2018), and evaluation is reported as mAP over all HOI classes. V-COCO

follows a similar protocol in 29 HOI classes defined on COCO images Lin et al. (2014). More recently, SWiG-HOI extends this principle to over 5,500 HOI classes, aiming for open-vocabulary HOI evaluation Wang et al. (2022). Although these benchmarks differ in label space, they all adopt exact-match protocols that require predictions to align strictly with annotated HOI classes. This is problematic in practice because annotations are often incomplete: some valid interactions are left unlabeled, especially in temporally ambiguous scenarios, and in multi-person scenes, the annotation is sparse for all possible human–object pairs in an image, which ultimately penalizes correct predictions.

Vision language models for HOI. Recent large VLMs have become the frontier of general-purpose image understanding Bai et al. (2025); Zhu et al. (2025); Liu et al. (2024); Shahriar et al. (2024); OpenAI (2023); Yang et al. (2023) . Although not explicitly trained for HOI detection, they show strong open-vocabulary grounding, spatial and visual reasoning abilities, making them natural candidates for studying HOI understanding. However, their capabilities have not been evaluated in HOI detection, and directly applying traditional HOI benchmarks (e.g., HICO-DET, V-COCO) with exact-match-based mAP is unsuitable for VLMs. Since their generative nature produces valid interpretations beyond incomplete interaction labels in ambiguous cases, and sparse annotations in multi-person scenes leave many pairs unlabeled, both causing underestimated performance. Our benchmark avoids such issues by reformulating HOI detection as multiple-choice question with curated negatives, and introducing complementary settings that comprehensively evaluate different aspects of HOI understanding.

5 CONCLUSION

In this work, we revisit the evaluation of HOI detection in the era of large VLMs. We showed that existing benchmarks such as HICO-DET suffer from incomplete annotations in two perspectives: missing interaction labels, mainly caused by temporal ambiguity and sparse annotations in multi-person scenes, both of which lead to underestimated performance, particularly for VLMs. To address these issues, we introduced the first benchmark that reformulates HOI detection as a multiple-answer, multiple-choice task with carefully curated negatives, ensuring that valid but unlabeled interactions are not penalized. Furthermore, we designed three complementary evaluation settings to evaluate different aspects of HOI tasks while mitigating the impact of sparse annotations: holistic HOI recognition across the whole scene with curated negatives to avoid penalizing unlabeled pairs, individual HOI recognition excluding person detection errors, and the joint HOI detection–recognition evaluation. Our experiments across state-of-the-art VLMs and HOI-specific methods provide new insights: small VLMs already surpass specialized HOI methods in the recognition-only setting, while larger VLMs achieve superior performance over all settings. Nevertheless, their performance is still far from perfect, indicating substantial room for improvement. We hope this benchmark serves as a foundation for comprehensive HOI evaluation, guiding future progress in both HOI-specific modeling and the broader development of VLMs.

REFERENCES

Shuai Bai, Keqin Chen, Xuejing Liu, Jialin Wang, Wenbin Ge, Sibo Song, Kai Dang, Peng Wang, Shijie Wang, Jun Tang, Humen Zhong, Yuanzhi Zhu, Ming-Hsuan Yang, Zhaohai Li, Jianqiang Wan, Pengfei Wang, Wei Ding, Zheren Fu, Yiheng Xu, Jiabo Ye, Xi Zhang, Tianbao Xie, Zesen Cheng, Hang Zhang, Zhibo Yang, Haiyang Xu, and Junyang Lin. Qwen2.5-vl technical report. *CoRR*, abs/2502.13923, 2025. doi: 10.48550/ARXIV.2502.13923.

Yichao Cao, Qingfei Tang, Xiu Su, Song Chen, Shan You, Xiaobo Lu, and Chang Xu. Detecting any human-object interaction relationship: Universal hoi detector with spatial prompt learning on foundation models. *Advances in Neural Information Processing Systems*, 36, 2024.

Nicolas Carion, Francisco Massa, Gabriel Synnaeve, Nicolas Usunier, Alexander Kirillov, and Sergey Zagoruyko. End-to-end object detection with transformers. In *European conference on computer vision*, pp. 213–229. Springer, 2020.

Yu-Wei Chao, Yunfan Liu, Xieyang Liu, Huayi Zeng, and Jia Deng. Learning to detect human–object interactions. In *2018 ieee winter conference on applications of computer vision (wacv)*, pp. 381–389. IEEE, 2018.

Zhe Chen, Jiannan Wu, Wenhui Wang, Weijie Su, Guo Chen, Sen Xing, Muyan Zhong, Qinglong Zhang, Xizhou Zhu, Lewei Lu, et al. Internvl: Scaling up vision foundation models and aligning for generic visual-linguistic tasks. In *Proceedings of the IEEE/CVF Conference on Computer Vision and Pattern Recognition*, pp. 24185–24198, 2024.

Jia Deng, Wei Dong, Richard Socher, Li-Jia Li, Kai Li, and Li Fei-Fei. Imagenet: A large-scale hierarchical image database. In *2009 IEEE conference on computer vision and pattern recognition*, pp. 248–255. Ieee, 2009.

Agrim Gupta, Piotr Dollár, and Ross B. Girshick. LVIS: A dataset for large vocabulary instance segmentation. In *IEEE Conference on Computer Vision and Pattern Recognition, CVPR 2019, Long Beach, CA, USA, June 16-20, 2019*, pp. 5356–5364. Computer Vision Foundation / IEEE, 2019. doi: 10.1109/CVPR.2019.00550.

Zhi Hou, Xiaojiang Peng, Yu Qiao, and Dacheng Tao. Visual compositional learning for human-object interaction detection. In *Computer Vision–ECCV 2020: 16th European Conference, Glasgow, UK, August 23–28, 2020, Proceedings, Part XV 16*, pp. 584–600. Springer, 2020.

Zhi Hou, Baosheng Yu, Yu Qiao, Xiaojiang Peng, and Dacheng Tao. Detecting human-object interaction via fabricated compositional learning. In *Proceedings of the IEEE/CVF Conference on Computer Vision and Pattern Recognition*, pp. 14646–14655, 2021.

Zhi Hou, Baosheng Yu, and Dacheng Tao. Discovering human-object interaction concepts via self-compositional learning. In *European Conference on Computer Vision*, pp. 461–478. Springer, 2022.

Aaron Hurst, Adam Lerer, Adam P. Goucher, Adam Perelman, Aditya Ramesh, Aidan Clark, AJ Os-trow, Akila Welihinda, Alan Hayes, Alec Radford, Aleksander Madry, Alex Baker-Whitcomb, Alex Beutel, Alex Borzunov, Alex Carney, Alex Chow, Alex Kirillov, Alex Nichol, Alex Paino, Alex Renzin, Alex Tachard Passos, Alexander Kirillov, Alexi Christakis, Alexis Conneau, Ali Kamali, Allan Jabri, Allison Moyer, Allison Tam, Amadou Crookes, Amin Tootoonchian, Ananya Kumar, Andrea Vallone, Andrej Karpathy, Andrew Braunstein, Andrew Cann, Andrew Codispoti, Andrew Galu, Andrew Kondrich, Andrew Tulloch, Andrey Mishchenko, Angela Baek, Angela Jiang, Antoine Pelisse, Antonia Woodford, Anuj Gosalia, Arka Dhar, Ashley Pantuliano, Avi Nayak, Avital Oliver, Barret Zoph, Behrooz Ghorbani, Ben Leimberger, Ben Rossen, Ben Sokolowsky, Ben Wang, Benjamin Zweig, Beth Hoover, Blake Samic, Bob McGrew, Bobby Spero, Bogo Giertler, Bowen Cheng, Brad Lightcap, Brandon Walkin, Brendan Quinn, Brian Guarraci, Brian Hsu, Bright Kellogg, Brydon Eastman, Camillo Lugaressi, Carroll L. Wainwright, Cary Bassin, Cary Hudson, Casey Chu, Chad Nelson, Chak Li, Chan Jun Shern, Channing Conger, Charlotte Barette, Chelsea Voss, Chen Ding, Cheng Lu, Chong Zhang, Chris Beaumont, Chris Hallacy, Chris Koch, Christian Gibson, Christina Kim, Christine Choi, Christine McLeavey, Christopher Hesse, Claudia Fischer, Clemens Winter, Coley Czarnecki, Colin Jarvis, Colin Wei, Constantin Koumouzelis, and Dane Sherburn. Gpt-4o system card. *CoRR*, abs/2410.21276, 2024. doi: 10.48550/ARXIV.2410.21276. URL <https://doi.org/10.48550/arXiv.2410.21276>.

Sanghyun Kim, Deunsol Jung, and Minsu Cho. Locality-aware zero-shot human-object interaction detection. In *IEEE/CVF Conference on Computer Vision and Pattern Recognition, CVPR 2025, Nashville, TN, USA, June 11-15, 2025*, pp. 20190–20200. Computer Vision Foundation / IEEE, 2025.

Qinqian Lei, Bo Wang, and Robby T. Tan. Ez-hoi: Vlm adaptation via guided prompt learning for zero-shot hoi detection. In *The Thirty-eighth Annual Conference on Neural Information Processing Systems*, 2024a.

Qinqian Lei, Bo Wang, and Robby T Tan. Few-shot learning from augmented label-uncertain queries in bongard-hoi. In *Proceedings of the AAAI Conference on Artificial Intelligence*, volume 38, pp. 2974–2982, 2024b.

Qinqian Lei, Bo Wang, and Tan Robby T. Hola: Zero-shot hoi detection with low-rank decomposed vlm feature adaptation. In *In Proceedings of the IEEE/CVF international conference on computer vision*, 2025.

Ting Lei, Fabian Caba, Qingchao Chen, Hailin Jin, Yuxin Peng, and Yang Liu. Efficient adaptive human-object interaction detection with concept-guided memory. In *Proceedings of the IEEE/CVF International Conference on Computer Vision*, pp. 6480–6490, 2023.

Ting Lei, Shaofeng Yin, and Yang Liu. Exploring the potential of large foundation models for open-vocabulary hoi detection. In *Proceedings of the IEEE/CVF Conference on Computer Vision and Pattern Recognition (CVPR)*, pp. 16657–16667, June 2024c.

Ting Lei, Shaofeng Yin, Yuxin Peng, and Yang Liu. Exploring conditional multi-modal prompts for zero-shot hoi detection. In *European Conference on Computer Vision*, pp. 1–19. Springer, 2024d.

Bo Li, Yuanhan Zhang, Dong Guo, Renrui Zhang, Feng Li, Hao Zhang, Kaichen Zhang, Peiyuan Zhang, Yanwei Li, Ziwei Liu, and Chunyuan Li. Llava-onevision: Easy visual task transfer. *Trans. Mach. Learn. Res.*, 2025, 2025. URL <https://openreview.net/forum?id=zKv8qULV6n>.

Junnan Li, Dongxu Li, Caiming Xiong, and Steven Hoi. Blip: Bootstrapping language-image pre-training for unified vision-language understanding and generation. In *International Conference on Machine Learning*, pp. 12888–12900. PMLR, 2022.

Liulei Li, Wenguan Wang, and Yi Yang. Human-object interaction detection collaborated with large relation-driven diffusion models. *arXiv preprint arXiv:2410.20155*, 2024a.

Liulei Li, Jianan Wei, Wenguan Wang, and Yi Yang. Neural-logic human-object interaction detection. *Advances in Neural Information Processing Systems*, 36, 2024b.

Yue Liao, Aixi Zhang, Miao Lu, Yongliang Wang, Xiaobo Li, and Si Liu. Gen-vlkt: Simplify association and enhance interaction understanding for hoi detection. In *Proceedings of the IEEE/CVF Conference on Computer Vision and Pattern Recognition (CVPR)*, pp. 20123–20132, June 2022.

Tsung-Yi Lin, Michael Maire, Serge Belongie, James Hays, Pietro Perona, Deva Ramanan, Piotr Dollár, and C Lawrence Zitnick. Microsoft coco: Common objects in context. In *Computer Vision–ECCV 2014: 13th European Conference, Zurich, Switzerland, September 6–12, 2014, Proceedings, Part V 13*, pp. 740–755. Springer, 2014.

Haotian Liu, Chunyuan Li, Yuheng Li, Bo Li, Yuanhan Zhang, Sheng Shen, and Yong Jae Lee. Llava-next: Improved reasoning, ocr, and world knowledge, January 2024. URL <https://llava-vl.github.io/blog/2024-01-30-llava-next/>.

Yunyao Mao, Jiajun Deng, Wengang Zhou, Li Li, Yao Fang, and Houqiang Li. Clip4hoi: Towards adapting clip for practical zero-shot hoi detection. *Advances in Neural Information Processing Systems*, 36, 2024.

Yusuke Niitani, Takuya Akiba, Tommi Kerola, Toru Ogawa, Shotaro Sano, and Shuji Suzuki. Sampling techniques for large-scale object detection from sparsely annotated objects. In *2019 IEEE/CVF Conference on Computer Vision and Pattern Recognition (CVPR)*, pp. 6503–6511, 2019. doi: 10.1109/CVPR.2019.00667.

Shan Ning, Longtian Qiu, Yongfei Liu, and Xuming He. Hoiclip: Efficient knowledge transfer for hoi detection with vision-language models. In *Proceedings of the IEEE/CVF Conference on Computer Vision and Pattern Recognition*, pp. 23507–23517, 2023.

OpenAI. GPT-4 technical report. *CoRR*, abs/2303.08774, 2023. doi: 10.48550/ARXIV.2303.08774. URL <https://doi.org/10.48550/arXiv.2303.08774>.

Jeeseung Park, Jin-Woo Park, and Jong-Seok Lee. Viplo: Vision transformer based pose-conditioned self-loop graph for human-object interaction detection. In *Proceedings of the IEEE/CVF Conference on Computer Vision and Pattern Recognition*, pp. 17152–17162, 2023.

Pouya Pezeshkpour and Estevam Rhruschka. Large language models sensitivity to the order of options in multiple-choice questions. In Kevin Duh, Helena Gomez, and Steven Bethard (eds.), *Findings of the Association for Computational Linguistics: NAACL 2024*, pp. 2006–2017, Mexico City, Mexico, June 2024. Association for Computational Linguistics. doi: 10.18653/v1/2024.findings-naacl.130. URL <https://aclanthology.org/2024.findings-naacl.130/>.

Xian Qu, Changxing Ding, Xingao Li, Xubin Zhong, and Dacheng Tao. Distillation using oracle queries for transformer-based human-object interaction detection. In *Proceedings of the IEEE/CVF Conference on Computer Vision and Pattern Recognition*, pp. 19558–19567, 2022.

Alec Radford, Jong Wook Kim, Chris Hallacy, Aditya Ramesh, Gabriel Goh, Sandhini Agarwal, Girish Sastry, Amanda Askell, Pamela Mishkin, Jack Clark, et al. Learning transferable visual models from natural language supervision. In *International conference on machine learning*, pp. 8748–8763. PMLR, 2021.

Pranav Rajpurkar, Jian Zhang, Konstantin Lopyrev, and Percy Liang. Squad: 100,000+ questions for machine comprehension of text. In Jian Su, Xavier Carreras, and Kevin Duh (eds.), *Proceedings of the 2016 Conference on Empirical Methods in Natural Language Processing, EMNLP 2016, Austin, Texas, USA, November 1-4, 2016*, pp. 2383–2392. The Association for Computational Linguistics, 2016. doi: 10.18653/V1/D16-1264. URL <https://doi.org/10.18653/v1/d16-1264>.

Sakib Shahriar, Brady D. Lund, Nishith Reddy Mannuru, Muhammad Arbab Arshad, Kadhim Hayawi, Ravi Varma Kumar Bevara, Aashrith Mannuru, and Laiba Batool. Putting gpt-4o to the sword: A comprehensive evaluation of language, vision, speech, and multimodal proficiency. *Applied Sciences*, 14(17), 2024. ISSN 2076-3417. doi: 10.3390/app14177782.

Saksham Suri, Saketh Rambhatla, Rama Chellappa, and Abhinav Shrivastava. Sparsedet: Improving sparsely annotated object detection with pseudo-positive mining. In *In Proceedings of the IEEE/CVF international conference on computer vision*, pp. 6747–6758, 10 2023. doi: 10.1109/ICCV51070.2023.00623.

Masato Tamura, Hiroki Ohashi, and Tomoaki Yoshinaga. Qpic: Query-based pairwise human-object interaction detection with image-wide contextual information. In *Proceedings of the IEEE/CVF Conference on Computer Vision and Pattern Recognition*, pp. 10410–10419, 2021.

Danyang Tu, Wei Sun, Guangtao Zhai, and Wei Shen. Agglomerative transformer for human-object interaction detection. In *Proceedings of the IEEE/CVF International Conference on Computer Vision (ICCV)*, pp. 21614–21624, October 2023.

Guangzhi Wang, Yangyang Guo, Ziwei Xu, and Mohan Kankanhalli. Bilateral adaptation for human-object interaction detection with occlusion-robustness. In *Proceedings of the IEEE/CVF Conference on Computer Vision and Pattern Recognition*, pp. 27970–27980, 2024a.

Suchen Wang, Yueqi Duan, Henghui Ding, Yap-Peng Tan, Kim-Hui Yap, and Junsong Yuan. Learning transferable human-object interaction detector with natural language supervision. In *Proceedings of the IEEE/CVF Conference on Computer Vision and Pattern Recognition*, pp. 939–948, 2022.

Weiyun Wang, Zhe Chen, Wenhui Wang, Yue Cao, Yangzhou Liu, Zhangwei Gao, Jinguo Zhu, Xizhou Zhu, Lewei Lu, Yu Qiao, and Jifeng Dai. Enhancing the reasoning ability of multimodal large language models via mixed preference optimization. *arXiv preprint arXiv:2411.10442*, 2024b.

Mingrui Wu, Jiaxin Gu, Yunhang Shen, Mingbao Lin, Chao Chen, and Xiaoshuai Sun. End-to-end zero-shot hoi detection via vision and language knowledge distillation. In *Proceedings of the AAAI Conference on Artificial Intelligence*, volume 37, pp. 2839–2846, 2023.

Xi-Zhu Wu and Zhi-Hua Zhou. A unified view of multi-label performance measures. In Doina Precup and Yee Whye Teh (eds.), *Proceedings of the 34th International Conference on Machine Learning, ICML 2017, Sydney, NSW, Australia, 6-11 August 2017*, volume 70 of *Proceedings of Machine Learning Research*, pp. 3780–3788. PMLR, 2017. URL <http://proceedings.mlr.press/v70/wu17a.html>.

Zhengyuan Yang, Linjie Li, Kevin Lin, Jianfeng Wang, Chung-Ching Lin, Zicheng Liu, and Lijuan Wang. The dawn of lmms: Preliminary explorations with gpt-4v(ision). *CoRR*, abs/2309.17421, 2023. doi: 10.48550/ARXIV.2309.17421. URL <https://doi.org/10.48550/arXiv.2309.17421>.

Hangjie Yuan, Jianwen Jiang, Samuel Albanie, Tao Feng, Ziyuan Huang, Dong Ni, and Mingqian Tang. Rlip: Relational language-image pre-training for human-object interaction detection. *Advances in Neural Information Processing Systems*, 35:37416–37431, 2022.

Hangjie Yuan, Shiwei Zhang, Xiang Wang, Samuel Albanie, Yining Pan, Tao Feng, Jianwen Jiang, Dong Ni, Yingya Zhang, and Deli Zhao. Rlipv2: Fast scaling of relational language-image pre-training. In *Proceedings of the IEEE/CVF International Conference on Computer Vision*, pp. 21649–21661, 2023.

Frederic Z Zhang, Dylan Campbell, and Stephen Gould. Spatially conditioned graphs for detecting human-object interactions. In *Proceedings of the IEEE/CVF International Conference on Computer Vision*, pp. 13319–13327, 2021.

Frederic Z Zhang, Dylan Campbell, and Stephen Gould. Efficient two-stage detection of human-object interactions with a novel unary-pairwise transformer. In *Proceedings of the IEEE/CVF Conference on Computer Vision and Pattern Recognition*, pp. 20104–20112, 2022.

Song-Hai Zhang, Ruilong Li, Xin Dong, Paul Rosin, Zixi Cai, Xi Han, Dingcheng Yang, Haozhi Huang, and Shi-Min Hu. Pose2seg: Detection free human instance segmentation. In *2019 IEEE/CVF Conference on Computer Vision and Pattern Recognition (CVPR)*, pp. 889–898, 2019. doi: 10.1109/CVPR.2019.00098.

Chujie Zheng, Hao Zhou, Fandong Meng, Jie Zhou, and Minlie Huang. Large language models are not robust multiple choice selectors. In *The Twelfth International Conference on Learning Representations*, 2024. URL <https://openreview.net/forum?id=shr9PXz7T0>.

Jinguo Zhu, Weiyun Wang, Zhe Chen, Zhaoyang Liu, Shenglong Ye, Lixin Gu, Hao Tian, Yuchen Duan, Weijie Su, Jie Shao, Zhangwei Gao, Erfei Cui, Xuehui Wang, Yue Cao, Yangzhou Liu, Xingguang Wei, Hongjie Zhang, Haomin Wang, Weiye Xu, Hao Li, Jiahao Wang, Nianchen Deng, Songze Li, Yinan He, Tan Jiang, Jiapeng Luo, Yi Wang, Conghui He, Botian Shi, Xingcheng Zhang, Wenqi Shao, Junjun He, Yingtong Xiong, Wenwen Qu, Peng Sun, Penglong Jiao, Han Lv, Lijun Wu, Kaipeng Zhang, Huipeng Deng, Jiaye Ge, Kai Chen, Limin Wang, Min Dou, Lewei Lu, Xizhou Zhu, Tong Lu, Dahua Lin, Yu Qiao, Jifeng Dai, and Wenhui Wang. Internvl3: Exploring advanced training and test-time recipes for open-source multimodal models. *CoRR*, abs/2504.10479, 2025. doi: 10.48550/ARXIV.2504.10479. URL <https://doi.org/10.48550/arXiv.2504.10479>.

Cheng Zou, Bohan Wang, Yue Hu, Junqi Liu, Qian Wu, Yu Zhao, Boxun Li, Chenguang Zhang, Chi Zhang, Yichen Wei, et al. End-to-end human object interaction detection with hoi transformer. In *Proceedings of the IEEE/CVF conference on computer vision and pattern recognition*, pp. 11825–11834, 2021.

Time-sensitive HOI Classes			
boarding an airplane	breaking a baseball bat	catching a frisbee	catching a sports ball
controlling a tv	controlling a mouse	directing an airplane	directing a bus
dragging a suitcase	dragging a surfboard	dribbling a sports ball	exiting an airplane
flipping a skateboard	hitting a sports ball	hopping on a bicycle	hopping on a horse
hopping on a motorcycle	hopping on an elephant	kicking a sports ball	launching a boat
launching a kite	lifting a fork	losing an umbrella	moving a refrigerator
opening a backpack	opening a book	opening a bottle	opening a fire hydrant
opening a laptop	opening a microwave	opening a refrigerator	opening a scissors
opening a suitcase	opening a toilet	opening an oven	opening an umbrella
packing a suitcase	picking a banana	picking an apple	picking an orange
picking up a cake	picking up a donut	picking up a pizza	picking up a skateboard
picking up a skis	picking up a sports ball	picking up a suitcase	pulling a kite
pulling a tie	releasing a bird	serving a sports ball	setting a clock
setting an umbrella	sliding a pizza	squeezing an orange	swinging a baseball bat
swinging a tennis racket	swinging a remote	throwing a baseball bat	throwing a frisbee
throwing a sports ball	turning a motorcycle	tying a boat	tying a tie
waving a bus	wielding a baseball bat	wielding a knife	zipping a suitcase

Table 5: List of 68 HOI classes in HICO-DET that are closely related to time information and often ambiguous in static images, while videos can disambiguate the temporal process.

scenario	Class 1 F1	Class 2 F1	Class 3 F1	Macro-F1
Single-person	0.2	0.5	/	0.35
Multi-person	0.4	/	0.3	0.35
Overall	0.3	0.5	0.3	0.37

Table 6: Illustrative example where the overall scenario yields higher Macro-F1 than the single- or multi-person scenarios.

A TIME-SENSITIVE HOI CLASSES IN HICO-DET

Out of the 600 pre-defined HOI classes in HICO-DET, we identified 68 classes that are closely related to time information, where static images can be inherently ambiguous and may not fully capture the temporal dynamics of the interaction. This finding shows that the examples highlighted in our paper (e.g., a frisbee interaction that could be interpreted as either “throwing” or “catching.”) are not isolated incidents, but rather representative of a broader issue that affects a substantial portion of the benchmark. All these classes are listed in Table 5.

B ON THE HIGHER MACRO-F1 IN THE OVERALL SCENARIO

A somewhat counterintuitive phenomenon is that the overall scenario may yield a higher Macro-F1 than either the “Single-person” or “Multi-person” scenarios alone. This arises because the overall scenario is the union of both subsets, and Macro-F1 is computed as the average over all HOI classes that appear in the evaluation. We provide a detailed discussion below.

Assume there are three HOI classes considered for Macro-F1 calculation:

- Class 1 appears in both single- and multi-person scenarios, with scores a (single), b (multi), and c (overall). Since the overall scenario aggregates across both subsets, c lies between a and b : $\min(a, b) < c < \max(a, b)$.
- Class 2 appears only in the single-person and overall scenarios, with scores x (single) and x (overall).
- Class 3 appears only in the multi-person and overall scenarios, with scores y (multi) and y (overall).

The Macro-F1 in each scenario is therefore

$$\begin{aligned}\text{Macro-F1}_{\text{single}} &= \frac{1}{2}(a + x), \\ \text{Macro-F1}_{\text{multi}} &= \frac{1}{2}(b + y), \\ \text{Macro-F1}_{\text{overall}} &= \frac{1}{3}(c + x + y).\end{aligned}\tag{5}$$

The overall scenario outperforms both subsets when

$$\frac{c + x + y}{3} > \frac{a + x}{2}, \quad \frac{c + x + y}{3} > \frac{b + y}{2},\tag{6}$$

which is equivalent to the conditions $x > a + 2b - 2c$ and $y > 2a + b - 2c$. These inequalities can hold in practice, explaining why the overall scenario, though merely a union of the subsets, may yield a higher Macro-F1 than either the single- or multi-person scenario alone. We provide a specific example for illustration, as shown in Table 6. Although the single-person and multi-person scenarios each achieve 0.35 Macro-F1, the overall scenario reaches 0.37.

C DATASET LICENSES AND RELEASE

Licenses We use the HICO-DET dataset Chao et al. (2018), which is publicly released under a CC0: Public Domain license.

Data Release and Ethical Considerations We do not release data beyond the original HICO-DET dataset. Instead, our benchmark release will contain evaluation questions constructed on top of HICO-DET. Each question is associated with the corresponding image index in HICO-DET, and the ground-truth HOI annotations used in our evaluation. No images or raw annotations are redistributed and users are required to obtain HICO-DET separately under its original license. As our release only provides derived question–answer pairs and image index mappings, the risk of exposing personally identifiable information or offensive content is minimal. Consent considerations follow those of the original HICO-DET release, and we do not conduct an independent investigation of consent beyond the original dataset.